SAR Analysis of Hexagonal-Shaped Slot-Loaded Patch Antenna for Hyperthermia Application at 434 MHz

Azharuddin Khan[*] **and Amit K. Singh**

Abstract—In this article, a low-profile microstrip patch antenna using an FR-4 substrate with relative permittivity of 4.4 and thickness of 1.6 mm is designed. On the top of a substrate, it consists of one metallic hexagonal patch and a metallic-fed hexagonal ring tone, and the ground part of the structure is covered with orthogonal rectangular slots. The designed structure operates in the ISM band of 434 MHz, and the overall size of the antenna is $124 \times 124 \times 1.6\,\text{mm}^3$. The antenna provides a valid SAR input profile.

1. INTRODUCTION

Cancer has emerged as one of the most debilitating diseases in the world today. The most common topical treatments used to treat cancer are radiation and chemotherapy. But these remedies have so many negative side effects, so finding options that allow the affected person to fight the infection without side effects or signs and symptoms of radiation and chemotherapy is very important. Other clinical studies on hyperthermia in combination with radiotherapy or chemotherapy were mentioned [1].

Hyperthermia is one of the most exciting areas to study the biological effects and use of microwaves to treat cancer and tumors. In addition to radiofrequency/microwave hyperthermia antenna devices, electric energy has been combined without affecting human skin as an additional ionizing anti-cancer agent or chemo-cure agent for the upper and lower neck [2]. Several studies have shown a significant reduction in plant length while combining hyperthermia with alternative therapies. Excessive thermal hyperthermia as well as extremely focused ultrasound are being considered in advance for the use as alternative traditional surgical treatments [3]. In cancerous regions, energy is used to raise the temperature to 42–45°C.

Hyperthermia is generally expressed as localized electromagnetic (EM) exposure to the cancer cell. EM power supplies can also be used in hyperthermia treatment programs by applying energy to the abscesses to increase local temperature and ultimately remove or reduce those abscesses. Hyperthermia is generally designed to increase tissue temperature to between 40 and 44°C [4]. Extreme temperatures (42°C to 45°C) appear to inhibit the formation of cancer cell proteins and therefore improve plant control in the environment by altering cell structure or even killing these cells [5]. Curing hyperthermia is less complicated and safer than chemotherapy or radiation therapy. However, the challenges associated with dynamic awareness of the EM force do not always prevent the wide popularity of this technique [6]. In local hyperthermia, heat is applied to a small area of affected tissue, such as a tumor or cancer, using various EM energy delivery techniques to heat the tissue. Various types of energy can be used to install heaters, including microwave, radio frequency, and ultrasound [7].

Issues related to the hyperthermia antenna structure are different from the antenna design for air and should not be ignored [8]. On the one hand, the antenna radiation reaches a lossy medium, which has a significant impact on the characteristics of the antenna [9, 10]. Therefore, the antenna design

* Corresponding author: Azharuddin Khan (azharuddin.khan.rs.ece18@iitbhu.ac.in).
The authors are with the Department of Electronics Engineering, IIT (BHU), Varanasi 221005, India.

methods found in the literature on lossless media were inappropriate, while experimental measurements need to be performed to verify the simulations in the case of hyperthermia antennas. In the case of deep hyperthermia (DHT) treatment, an elliptical or circular array with multiple antennas is used, which are attached to the patient with a water bolus filled with demineralized water. The water bolus application guarantees an antenna design that affects efficient radiation emanating from the patch antenna material into the water bolus [11].

Despite the increased interest in cancer treatment in recent years, there are only a few research articles in the past on the microstrip patch antenna with a planar phantom. The novelty of this proposed antenna lies in obtaining the ISM band of 434 MHz with a comparable value of SAR. In this paper, a hexagon-shaped microstrip patch antenna is simulated, fabricated, and measured to study the Specific Absorption Rate (SAR) performance which will extend further for Hyperthermia applications.

2. MATERIAL AND METHODS

2.1. Antenna Geometry

In this section, a hexagonal microstrip patch is designed to cover the ISM band of 434 MHz using an FR-4 substrate (dielectric constant $\varepsilon_r = 4.4$, thickness $h = 1.6$ mm, and loss tangent $\tan \delta = 0.02$). The hexagonal patch of major radius $R1 = 30$ mm, a concentric annular ring of inner major radius $R2 = 40$ mm, and outer major radius $R3 = 50$ mm, on the dielectric substrate. Dimensions of the hexagon patch were given from a set of Equations (1)–(3) [12]. The proposed antenna configuration is illustrated in Figure 1. The ground side is covered by two rectangular orthogonal slots of different lengths and the same widths (w) combined with a square slot of side (a) positioned behind the center of the patch. Dimensions of the slots were given from a set of Equations (4)–(9) [13, 14]. Slots in the ground plane act like a load that can be used to bring the input impedance point closer to the characteristic impedance when being added to the antenna. The geometrical parameters of the proposed structure are shown in Table 1. A 50-ohm coaxial feed is applied inside the annular ring with an inner radius of
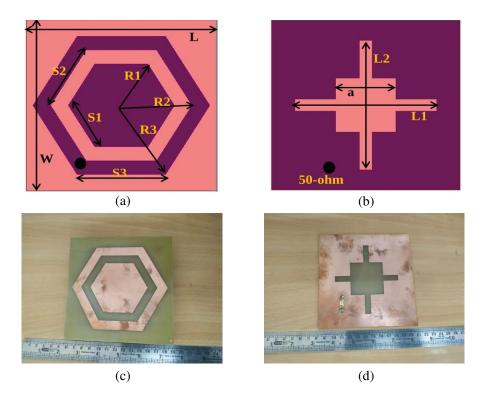

Figure 1. The geometrical configuration of the proposed antenna. (a) Top view. (b) Bottom view. (c) Fabricated antenna top view. (d) Fabricated antenna bottom view.

Table 1. Geometrical parameters of the proposed antenna.

Parameter	Value (mm)	Parameter	Value (mm)
L	124	$S1$	34.641
W	124	$S2$	46.188
L_1	93	$S3$	57.735
L_2	94	R_{in}	0.47
a	38.5	w	8

$0.47\,\mathrm{mm}$ to power-fed the antenna. Single-layered TEL (tissue equivalent liquid) planar phantom has been taken into consideration throughout the procedure.

The resonant frequency for the lowest order mode is given as [12],

$$\beta S = 2.01 \tag{1}$$

The equivalent radius of a hexagon patch is given as [12],

$$\pi R_{eq}^2 = \frac{3\sqrt{3}S^2}{2} \tag{2}$$

Thus,

$$f_r = \frac{K_{nm}c}{2\pi(R_{eq})\sqrt{\varepsilon_r}} \tag{3}$$

where β is the phase constant, S the side of the hexagon, K_{nm} the mth zero of the derivative of the Bessel function of order n, and c the velocity of light in free space.

Mathematical calculation for the slot on ground plane is taken from [13, 14].

When a slot is embedded in a patch, having dimension $(L_s \times W_s)$, it can be analyzed by using the duality relationship between the dipole and slot [14].

The radiation resistance of the slot is given as,

$$R_r = \frac{\eta \cos^2\alpha}{2\pi} \int_0^\pi \left[\frac{\cos\dfrac{k^2\cos\theta}{2} - \cos\dfrac{kL_s}{2}}{\sin\theta} \right] d\theta \tag{4}$$

The total input impedance of the slot is as,

$$Z_{\text{slot}} = \frac{\eta^2}{4Z_{cy}} \tag{5}$$

where Z_{cy} is given as

$$Z_{cy} = R_r(kL_s) - \mathrm{j}\left\{ 120\left(\ln\left(\frac{L_s}{W_s}\right) - 1 \right) \cot\frac{kL_s}{2} - X_r(kL_s) \right\} \tag{6}$$

where R_r is the real part and equivalent to the radiation resistance of the slot, and X_r is the input reactance of the slot and given as,

$$X_r = 30\cos^2\alpha\left\{ 2S_i(kL_s) + \cos(kL_s)\left[2S_i(kL_s) - S_i(2kL_s) - \sin(kL_s)\right] \right.$$
$$\left. \left[2C_i(kL_s) - C_i(2kL_s) - C_i\left(\frac{2kW^2}{L_s}\right) \right] \right\} \tag{7}$$

where $S_i(x)$ and $C_i(x)$ are the sine and cosine integrals defined as,

$$S_i(x) = \int_0^x \frac{\sin(x)}{x}\,dx \tag{8}$$

$$C_i(x) = -\int_0^\infty \frac{\sin(x)}{x}\,dx \tag{9}$$

2.2. TEL Single Layered Phantoms Tissue Model

Three layered phantom tissue model with water bolus has been taken as per IEEE standards. Water bolus layered has different significances for taking it into consideration makes the EM field transmission into the phantom with less reflection from the surface. It is also used for cooling down the skin layer at constant temperature, and one more interesting function of water bolus layer is to protect the EM field radiation at a safety level. The relative permittivity of each layer is different. We have to make a single-layer phantom as per measurement availability in a laboratory. Effective permittivity for single layer phantom tissue model is given in Equation (10).

$$\epsilon_{eff} = \left(\epsilon_{r1} + \epsilon_{r2}\right)/2 \tag{10}$$

where ϵ_{r1} and ϵ_{r2} are relative permittivities of different layers, using the above equation to calculate the effective permittivity of phantom tissue. The model overloads the antenna fields and provides the main SAR pattern due to the combined strength. Dielectric parameters, permittivity (ϵ_r), are 64.28; conductivity (σ) is 0.253 S/m; and density (ρ) is 1100 kg/m^3 in the ISM band [15, 16]. The size of cubical phantoms is $190 \times 130 \times 50$ mm^3 taken into consideration for simulation as well as during measurement. The height of the tissues layered was limited to 50 mm, and due to relatively moderate losses, fat tissue does not significantly contribute to the averaged SAR [17]. To account for extra variations [15], we have varied the distance from 3 cm to 9 cm with a step size of 3 cm between the antenna and phantom.

3. RESULTS AND DISCUSSION

3.1. Reflection Coefficient (S_{11})

Figure 2(a) shows the comparison of simulated v/s measured reflection coefficient with and without phantom. The simulated value of the reflection coefficient is -22.3 dB, and the measured value of the reflection coefficient is -21.1 dB in the case of without phantom. In the case of the TEL phantom simulated and measured reflection coefficients at a 3 cm distance between the phantom and antenna are 12.1 dB and -8.9 dB, respectively. The differences between the simulated and measured results can be attributed to the manufacturing tolerances, quality of the SMA connector, and scattering environment. For reflection coefficient measurement shown in Figure 2(b), the antenna is directly connected to a spectrum analyzer (R&S FSH8 100 kHz–8 GHz) with a probe.
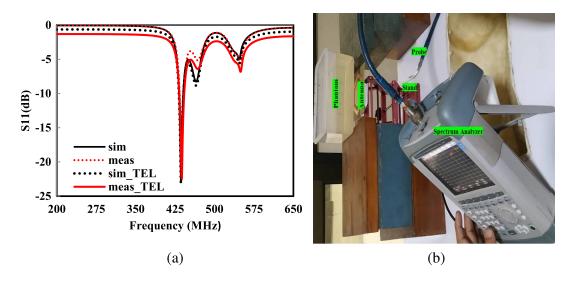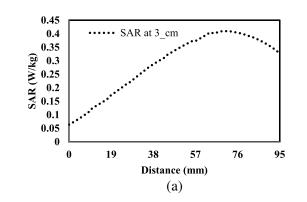

(a)   (b)

Figure 2. (a) Simulated and measured S_{11} with TEL phantom and without phantom. (b) Measurement of S_{11}.

3.2. Specific Absorption Rate (SAR)

The specific absorption rate is a measure of the amount of power deposited by a radio frequency field in a certain mass of tissue. Figure 3(a) shows the simulated SAR value of 0.4 W/kg along the x-axis at a 3 cm phantom distance from the antenna. SAR is determined by measuring Electric Field (E) inside the TEL Phantom shown in Figure 3(b). Fix the antenna and phantom positions at a 3 cm distance. Set the power level of the SMR signal generator (R&S SMB100A 10 MHz–40 GHz) is 0 dBm, i.e., 1 mw, set the operating frequency 434 MHz, and connect the probe to the antenna. Now set the same frequency in the spectrum analyzer and connect one port with the Electric Probe [18, 19] and another port to the computer. Now, Electric Probe [18] is inserted into the TEL phantom to different positions along the variation of the x-axis for electric field reading. After getting the electric field value, SAR will be calculated by Equation (11) in terms of electric field, conductivity, and density of the tissue, and results are summarized in Table 2.

$$\mathrm{SAR} = \frac{\sigma E^2}{2\rho} \,(\mathrm{W/kg}) \tag{11}$$

From Table 3 it can be concluded that the proposed antenna operates at 434 MHz with a reflection coefficient of -22.3 dB and shows a better SAR value of 0.4 W/kg than the antenna structures reported in [11, 20, 21].
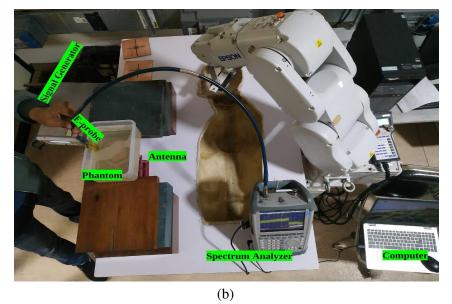

(a)

(b)

Figure 3. (a) Simulated SAR value along the x-axis at a 3 cm distance between TEL phantom and antenna. (b) Measurement of electric field.

Table 2. Calculated SAR value when the E-fields were measured along the x-axis.

Phantom Detail	Distance b/w antenna and Phantom (d) in cm	Distance inside the Phantom (x_1) in cm	Measured E-Field at (x_1) V/m	SAR (W/kg)
TEL	3	5.0	44.75	0.2303
		6.5	45.26	0.2355
		8.0	45.89	0.2422
		9.5	46.57	0.2494

Table 3. Qualitative comparison of reported antennas to the proposed antenna.

Ref.	Freq.	S_{11} (dB)	SAR (W/kg)	Size (mm)	Area (cm^2)	Application
[11]	434 MHz	−13.8	1.32	$130 \times 130 \times 2.97$	169	MICS
[20]	434 MHz	−16	1.32	$124 \times 124 \times 1.6$	153.76	MICS
	915 MHz	−17	1.44			
[21]	915 MHz	−32	11.17	$120 \times 120 \times 2.007$	144	MICS
	2.45 GHz	−27	27.93			ISM
work	434 MHz	−22.3	0.4	$124 \times 124 \times 1.6$	163.84	MICS

4. CONCLUSION

In this work, a hexagonal patch antenna is designed at 434 MHz for hyperthermia application. The antenna performance is compared at different distances from the phantom model using finite element method (FEM) modeling. SAR and reflection coefficient are evaluated at a 3 cm distance from the phantom. The value of SAR lies in the permissible limit of the exposed body as stated by IEEE standards.

ACKNOWLEDGMENT

REFERENCES

1. Correia, D., H. Petra Kok, M. de Greef, A. Bel, N. van Wieringen, and J. Crezee, "Body conformal antennas for superficial hyperthermia: The impact of bending contact flexible microstrip applicators on their electromagnetic behavior," *IEEE Transactions on Biomedical Engineering*, Vol. 56, No. 12, 2917–2926, 2009.

2. Horsman, M. R. and J. Overgaard, "Hyperthermia: A potent enhancer of radiotherapy," *Clinical Oncology*, Vol. 19, No. 6, 418–426, Aug. 2007.

3. Van Esser, S. and R. Van Hillegersberg, "Minimally invasive ablative therapies for invasive breast carcinomas: An overview of current literature," *World J. Surg.*, Vol. 31, 2284–2292, 2007.

4. Yang, X., J. Du, and Y. Liu, "Advances in hyperthermia technology," *Proceedings of the 2005 IEEE Engineering in Medicine and Biology 27th Annual Conference*, Shanghai, China, Sep. 2005.

5. Islk, O., E. Korkmaz, and B. Tiiretken, "Antenna arrangement considerations for microwave hyperthermia applications," *General Assembly and Scientific Symposium*, 2011.

6. Neufeld, E., M. Pauildes, M. Capstick, G. V. Rhoon, and N. Kuster, "Recent advances in hyperthermia cancer treatment," *Asia-Pacific International Symposium on Electromagnetic Compatibility*, Beijing, China, Apr. 2010.

7. Van der Zee, J., "Heating the patient: A promising approach," *Annals of Oncology*, Vol. 13, No. 8, 1173–1184, 2002.

8. Stauffer, P. R., "Evolving technology for thermal therapy of cancer," *Int. J. Hyperthermia*, Vol. 21, 731–744, 2005.

9. Hand, J. W. and J. R. James, *Physical Techniques in Clinical Hyperthermia*, Ch. 4, Research Studies Press, Letchworth, U.K., 1986.

10. King, R. W. P., B. S. Trembley, and J. W. Strohbein, "The electromagnetic field of an insulated antenna in a conducting or dielectric medium," *IEEE Trans. Microw. Theory Tech.*, Vol. 31, No. 7, 574–583, Jul. 1983.

11. Curto, S., P. McEvoy, X. Bao, and M. J. Ammann, "Compact patch antenna for electromagnetic interaction with human tissue at 434 MHz," *IEEE Trans. Antennas Propag.*, Vol. 57, No. 9, 2564–2571, 2009.

12. Bahl, I. J., P. Bhartia, and P. Bhartia, *Microstrip Antennas*, Artech House, 1980.

13. Ansari, J., A. Mishra, and B. Vishvakarma, "Half U-slot loaded semicircular disk patch antenna for GSM mobile phone and optical communications," *Progress In Electromagnetics Research C*, Vol. 18, 31–45, 2011.

14. Wolf, E. A., *Antenna Analysis*, Artech House, Narwood, USA, 1998.

15. Curto, S. and M. J. Ammann, "Electromagnetic coupling mechanism in a layered human tissue as a benchmark for 434 MHz RF hyperthermia applicators," *Proc. IEEE Antennas Propag. Society Int. Symp.*, 3185–3188, Honolulu, HI, Jun. 2007.

16. Christ, A., A. Klingenbock, T. Samaras, C. Goiceanu, and N. Kuster, "The dependence of electromagnetic far-field absorption on body tissue composition in the frequency range from 300 MHz to 6 GHz," *IEEE Trans. Microw. Theory Tech.*, Vol. 54, No. 5, 2188–2195, May 2006.

17. Christ, A., T. Samaras, A. Klingenbock, and N. Kuster, "Characterization of the electromagnetic near-field absorption in layered biological tissue in the frequency range from 30 MHz to 6000 MHz," *Phys. Med. Biol.*, Vol. 51, No. 19, 4951–4965, Sep. 2006.

18. Narang, N., S. K. Dubey, P. S. Negi, and V. N. Ojha, "Precise E-field measurement inside TEM cell at GSM frequencies using microstrip E-field probe," *2016 International Conference on Signal Processing and Communication (ICSC)*, IEEE, 2016.

19. Narang, N., S. K. Dubey, P. S. Negi, and V. N. Ojha, "A coplanar microstrip antenna as a dosimetric E-field probe for GSM frequencies," *MAPAN*, Vol. 32, No. 2, 143–147, 2017.

20. Younesiraad, H., M. Bemani, and S. Nikmehr, "A dual-band slotted square ring patch antenna for local hyperthermia applications," *Progress In Electromagnetics Research Letters*, Vol. 71, 97–102, 2017.

21. Halheit, H., A. V. Vorst, S. Tedjini, and R. Touhami, "Flexible dual-frequency applicator for local hyperthermia," *International Journal of Antennas and Propagation*, Vol. 2012, 1–7, 2012.